Carbohydrate Reaction Intermediates: Effect of Ring-Oxygen Protonation on the Structure and Conformation of Aldofuranosyl Rings

Jamie Kennedy,[†] Jian Wu,[‡] Kenneth Drew,[†] Ian Carmichael,[§] and Anthony S. Serianni*,[†]

Contribution from the Department of Chemistry and Biochemistry, University of Notre Dame, Notre Dame, Indiana 46556, Department of Human Biological Chemistry and Genetics, University of Texas Medical Branch, Galveston, Texas 77555-1157, and Radiation Laboratory, University of Notre Dame, Notre Dame, Indiana 46556

Received October 28, 1996. Revised Manuscript Received June 11, 1997[⊗]

Abstract: The effect of ring-oxygen protonation on the structure and conformational properties of a model deoxyaldofuranose, 2-deoxy-*β*-D-*glycero*-tetrofuranose **2**, has been examined with the use of NMR spectroscopy and *ab initio* molecular orbital calculations conducted at the HF/6-31G* level of theory. The computational method was validated by comparing the conformational behavior of **2** derived from PSEUROT treatment of $^3J_{HH}$ values measured in **2** (^2H_2O solvent) with that predicted from the theoretical calculations. Coupling data indicate that **2** favors S forms in solution (∼89% $^4T_3$, ∼11% E_2), while MO data indicated more comparable populations of the same or very similar N and S forms. Protonation of **2** at the ring oxygen (O4), yielding **1**, gave two distinct protonated forms which differed in the orientation of the proton about O4. Both forms showed substantial changes in ring structure and conformation compared to **2**. Protonated forms almost exclusively prefer S forms (E_3), and energy barriers for N/S interconversion were found to be considerably higher than those for **2**, leading to the conclusion that **1** is more conformationally constrained than **2**. Bond lengths in the vicinity of O4 changed significantly upon conversion of **2** to **1**; for example, the C1−O4 bond length increases by ∼14%, the C1−H1 and C1−O1 bond lengths decrease by 1−5%, and the C4−O4 bond length increases by ∼5%. These results indicate that O4 protonation predisposes **2** toward ring opening by inducing specific structural and conformational modifications, thus providing a more concise explanation of the role of acid catalysis in furanose anomerization (*i.e.*, **1** resembles the transition state of the acid-catalyzed anomerization reaction more than **2**). The molecular orbital data obtained in this investigation also provide evidence for a new structural factor (a 1,3-effect involving oxygen lone-pair orbitals) that influences bond lengths in carbohydrates.

Introduction

Furanosyl rings are common scaffolds upon which many biologically-important compounds, both simple and complex, are constructed. For example, cell metabolites such as D-fructose 1,6-bisphosphate and D-ribose 5-phosphate contain a single furanose ring, whereas biopolymers such as nucleic acids and some polysaccharides (*e.g.*, inulin) are comprised of many furanose building blocks. In contrast to most pyranosyl rings,[1] furanosyl rings are not conformationally homogeneous in solution, but exist in various nonplanar envelope and twist conformers that are similar in energy (energy barriers < ∼4 kcal/mol).[2] The spontaneous interconversion between these forms in solution proceeds via a pseudorotational itinerary[2a] (Figure 1) in which nonplanar forms (E, envelope; T, twist) interconvert with other nonplanar forms, that is, the less stable planar form is not involved as an intermediate. An alternative, and presumably less preferred, mode of conformer exchange (*i.e.*, inversion) describes conformer interconversion via the planar form.[2c]

The fluxional behavior of furanosyl rings confers considerable flexibility to molecules that contain them, and this flexibility may have important implications for biological recognition. For example, given the relative ease of interconversion of nonplanar furanose conformers, it is energetically possible that conformational change may occur in substrates containing a furanose constituent upon initial binding by enzymes. In contrast, conformational change is less likely for most pyranosyl rings, at least for $^4C_1$ and $^1C_4$ interconversion, where the energy barrier for interconversion is considerably greater.[2e] Likewise, chemistry performed on a furanose ring during an enzyme-catalyzed reaction might be accompanied by significant change in ring shape, again facilitated by the low barriers for conformer interconversion. These changes, if they occur, might represent an important element in the underlying molecular processes affecting catalytic efficiency. Indeed, such structural and/or conformational changes have been implicated in transition state analyses of enzyme reactions involving oxycarbonium ion intermediates derived from furanose-containing substrates.[3]

* Address correspondence to this author.
[†] Department of Chemistry and Biochemistry, University of Notre Dame.
[‡] Department of Human Biological Chemistry and Genetics, University of Texas Medical Branch.
[§] Radiation Laboratory, University of Notre Dame.
[⊗] Abstract published in *Advance ACS Abstracts,* August 1, 1997.

(1) Many aldopyranosyl rings, such as those having the *gluco, manno,* and *galacto* configurations, are considered highly conformationally constrained to a single chair form (*e.g.*, $^4C_1$ for D-*gluco*). In contrast, a few rings, such as those having the *ribo, ido,* and *altro* configurations, exhibit considerable conformational mobility.

(2) (a) Altona, C.; Sundaralingam, M. *J. Am. Chem. Soc.* **1972**, *94*, 8205−8212. (b) Harvey, S. C.; Prabhakaran, M. *J. Am. Chem. Soc.* **1986**, *108*, 6128−6136. (c) Westhof, E.; Sundaralingam, M. *J. Am. Chem. Soc.* **1983**, *105*, 970−976. (d) Levitt, M.; Warshel, A. *J. Am. Chem. Soc.* **1978**, *100*, 2607−2613. (e) The free energy barrier for chair interconversion of cyclohexane has been estimated at ∼10 kcal/mol (Jensen, F. R.; Noyce, D. S.; Sederholm, C. H.; Berlin, A. J. *J. Am. Chem. Soc.* **1962**, *84*, 386); barriers for aldopyranose chair interconversion are expected to be considerably higher (Dowd, M. K.; French, A. D.; Reilly, P. J. *Carbohydr. Res.* **1994**, *264*, 1−19).

S0002-7863(96)03727-4 CCC: $14.00

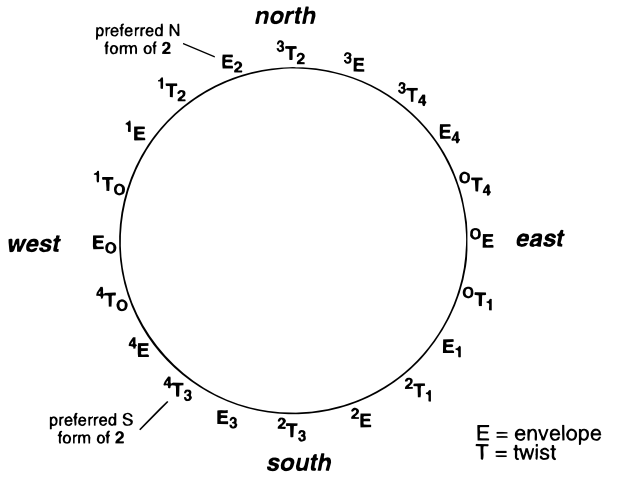

Figure 1. The pseudorotational itinerary of an aldofuranose ring. The preferred north (N) and south (S) conformers of **2**, derived from $^3J_{HH}$ analysis by PSEUROT 6.2,[11] are E_2 and $^4T_3$, respectively, as shown.

Scheme 1

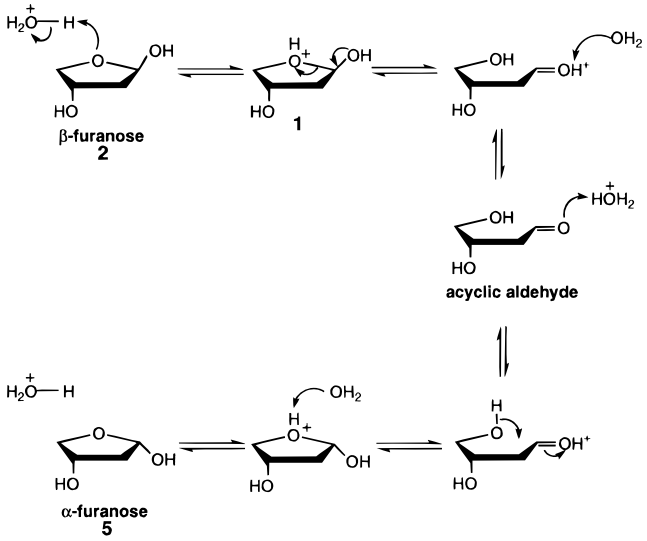

In solution, monosaccharides undergo spontaneous anomerization to generate an equilibrium mixture of furanose, pyranose, and acyclic forms.[4] The reaction in aqueous solution is catalyzed by acid, base, or water.[4a−c] The acid-catalyzed reaction is believed to involve the initial protonation of the ring oxygen and subsequent endocyclic C−O bond cleavage to generate the acyclic carbonyl form (Scheme 1). Analogous protonation reactions may be involved in enzyme-mediated reactions, such as those catalyzed by anomerases and glycosidases;[5] in the latter case, protonation is presumed to occur at the glycosidic oxygen, leading to the generation of an oxycarbonium ion intermediate. In light of the importance of protonation events in carbohydrate chemistry and biochemistry in general, we have examined the effect of ring-oxygen protonation on the structure and conformation of a model deoxyaldofuranose, 2-deoxy-β-D-*glycero*-tetrofuranose **2** (Scheme 1).

The solution structure of 2-deoxy-β-D-*glycero*-tetrofuranose **2** protonated at O4 (**1** in Scheme 1) cannot be studied directly via experimental methods such as NMR spectroscopy since **1** cannot be generated at concentrations sufficient for detection. However, the structure of **1** can be assessed in principle by computational methods. This study examines the effect of ring-oxygen protonation on the structure of 2-deoxy-β-D-*glycero*-tetrofuranose **2** (Scheme 1) with use of *ab initio* molecular orbital methods. We first provide experimental validation of the computational approach by comparing the solution behavior of **2** determined by NMR spectroscopy to that predicted by computation. We then assess the structural changes that occur upon O4 protonation of **2** and discuss potential implications of the observed changes for chemical and biological processes where a similar protonation event might occur.

Experimental Section

Preparation of 2-Deoxy-D-*glycero*-tetrose 3. 2-Deoxy-D-*glycero*-tetrose **3** was prepared by treating 3-deoxy-D-*erythro*-pentose (3-deoxy-D-ribose, **4**)[6] with $Pb(OAc)_4$ as described previously.[7] Crude **3** isolated

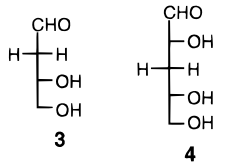

from the glycol scission reaction was purified by chromatography on Dowex 50 × 8 (200−400 mesh) ion-exchange resin in the Ca^{2+} form.[8] Column fractions were assayed with phenol−sulfuric acid,[9] and fractions containing **3** were combined, deionized by batch treatment with Dowex 50 × 8 (H^+) and Dowex 1 × 8 (OAc^-) ion-exchange resins, and concentrated to give a dilute aqueous solution of **3**.[10] A portion of this solution containing ~0.1 mmol of **3** was concentrated *in vacuo* at 30 °C to a syrup, and the latter was immediately dissolved in ^2H_2O (2−4 mL) (98.9 atom % ^2H; Cambridge Isotope Laboratories) and evaporated to dryness; this exchange was repeated twice more, and the final solution (~30 mM in ^2H_2O) was transferred to a 5-mm NMR tube.

NMR Spectroscopy. The 1D ^1H NMR spectrum of **3** in ^2H_2O at ~25 °C was obtained on a Varian Unity*Plus* 750-MHz NMR spectrometer (750.252 MHz for ^1H) at the Department of Human Biological Chemistry and Genetics, University of Texas Medical Branch, Galveston, TX. Spectral data were resolution enhanced to facilitate the observation and assignment of signals, and the extraction of $^1H-^1H$ spin-coupling constants. $^3J_{HH}$ values were fit to a two-state N/S pseudorotational model using PSEUROT 6.2,[11a] which applies a parametrized Karplus equation[11b,12ab] to the coupling data and yields pseudorotational phase angles (P) and puckering amplitudes (τ_m) for the preferred north (N) and south (S) forms, and the percentage of S

(3) (a) Horenstein, B. A.; Schramm, V. L. *Biochemistry* **1993**, *32*, 7089−7097. (b) Parkin, D. W.; Mentch, F.; Banks, G. A.; Horenstein, B. A.; Schramm, V. L. *Biochemistry* **1991**, *30*, 4586−4594.

(4) (a) Pigman, W.; Isbell, H. S. *Adv. Carbohydr. Chem. Biochem.* **1968**, *23*, 11. (b) Isbell, H. S.; Pigman, W. *Adv. Carbohydr. Chem. Biochem.* **1969**, *24*, 13. (c) Capon, B.; Walker, R. B. *J. Chem. Soc., Perkins Trans. 2* **1974**, *2*, 1600-1610. (d) Serianni, A. S.; Pierce, J.; Huang, S.-G.; Barker, R. *J. Am. Chem. Soc.* **1982**, *104*, 4037−4044. (e) Snyder, J. R.; Johnston, E. R.; Serianni, A. S. *J. Am. Chem. Soc.* **1989**, *111*, 2681−2687.

(5) (a) Sinnott, M. L. *Chem. Rev.* **1990**, *90*, 1171. (b) Legler, G. *Adv. Carbohydr. Chem. Biochem.* **1990**, *48*, 319.

(6) Witczak, Z. J.; Whistler, R. L. *Carbohydr. Res.* **1982**, *110*, 326−329.

(7) Snyder, J. R.; Serianni, A. S. *Carbohydr. Res.* **1991**, *210*, 21−38.

(8) Angyal, S. J.; Bethell, G. S.; Beveridge, R. J. *Carbohydr. Res.* **1979**, *73*, 9−18.

(9) Hodge, J. E.; Hofreiter, B. T. *Methods Carbohydr. Chem.* **1962**, *1*, 380.

(10) Concentration of aqueous solutions of **3** to a syrup was avoided to prevent the formation of oligomers, which is common in concentrated solutions of short-chain aldoses.

(11) (a) PSEUROT 6.2, Gorlaeus Laboratories, University of Leiden. (b) The PSEUROT 6.2 calculations on **2** were conducted using the $^3J_{HH}$ data given in Table 1. The input parameters (phase, A_i, B_i, S1, S2, S3, and S4) for each of the six couplings were determined by using the recommended values in Tables 3 and 5 in the program documentation. Couplings were fit by using the generalized Karplus equation (Donders, L. A.; de Leeuw, F. A. A. M.; Altona, C. *Magn. Reson. Chem.* **1989**, *27*, 556). The three *cis*-coupling constants in **2** ($^3J_{H1,H2R}$, $^3J_{H2S,H3}$, $^3J_{H3,H4R}$) were corrected for the Barfield transmission effect by using the correction parameters, P_b and T_b, recommended in Table 2 of the program documentation. In the present calculation, deviations between the observed and computed couplings ranged from 0.02 to 0.34 Hz (the maximum deviation was observed for $^3J_{H1,H2R}$), producing an overall root-mean-square deviation of 0.18 Hz.

Chart 1

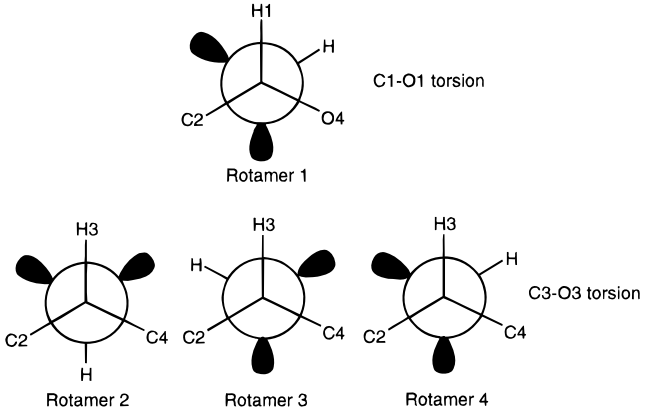

Chart 2

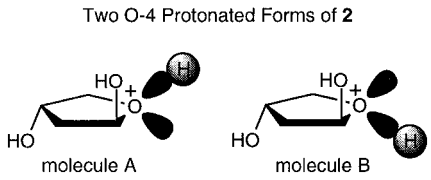

form in solution. Pseudorotational phase angles (P) divided by π give values ranging from 0−2 radians, which correspond to specific E and T forms (*e.g.*, $P/\pi = 0.1$ for ^{3}E, $P/\pi = 0.3$ for E_4, and so forth) (Figure 1).

Molecular Orbital Calculations. *Ab initio* molecular orbital calculations were performed by using the Gaussian 92 suite of programs.[13] Ten envelope (E) and the planar forms of **2** were examined at the HF/6-31G* level of theory by restricting one endocyclic torsion angle to 0° (two endocyclic torsions were held at 0° in the planar form) as described previously.[14] The initial C1−O1 torsion angle was set to optimize the "exoanomeric effect"[15] (Rotamer 1, Chart 1); the initial C3−O3 torsion angle was set to one of three possible values (Rotamers 2−4, Chart 1) to examine the effect of this torsion on calculated structures and energies of **2**. Similar calculations were performed on **1**; however, in this case, only one combination of exocyclic C−O torsions was examined (Rotamers 1 and 3, Chart 1). Preliminary calculations showed that two distinct geometries about O4 in optimized structures of **1** were possible (Chart 2), and thus two sets of calculations were performed to assess the differences between these forms (hereafter referred to as molecules A and B; Chart 2).

Results and Discussion

A. Validation of the Computational Method. Since an experimental (NMR) determination of the solution behavior of **1** is not feasible, we first assessed the solution properties of **2** by ^{1}H NMR spectroscopy, and compared the conformational conclusions based on these data with those derived via molecular orbital calculations. This approach to validating the computational method assumes that the degree of consistency between the NMR and computational data for **2** will be similar to that for **1**.

Table 1. ^{1}H NMR Parameters for 2-Deoxy-β-D-*glycero*-tetrofuranose (**2**) in ^2H_2O

nucleus	chemical shift, δ (ppm)[a]	nucleus	chemical shift, δ (ppm)[a]
H1	5.639	H3	4.537
H2*R*	2.181	H4*R*	4.002
H2*S*	2.016	H4*S*	3.763
coupled nuclei	**coupling constant, J (Hz)[b]**	**coupled nuclei**	**coupling constant, J (Hz)[b]**
H1, H2*R*	5.7	H2*R*, H2*S*	−14.7
H1, H2*S*	4.2	H3, H4*R*	3.8
H2*R*, H3	1.8	H3, H4*S*	1.4
H2*S*, H3	5.9	H4*R*, H4*S*	−10.1

[a] ±0.001 ppm, relative to H_2O (4.800 ppm). [b] ±0.1 Hz.

Chart 3

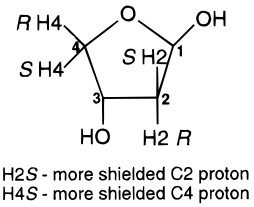

The 750-MHz ^{1}H NMR spectrum of 2-deoxy-D-*glycero*-tetrose **3** in ^2H_2O contains signals for the β-anomer **2** that are sufficiently disperse to permit a first-order analysis. Signals attributable to the α-furanose **5** and acyclic hydrate (*gem*-diol) **6** were also observed but not further analyzed. ^{1}H chemical shifts and ^{1}H−^{1}H spin-coupling constants obtained for **2** are given in Table 1.

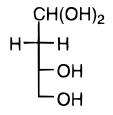

6

The six $^3J_{HH}$ values in **2** (Table 1) were fit to a two-state north−south (N/S) conformational model by using the PSEUROT 6.2 program,[11a] which yields preferred N and S forms (phase angles P_N and P_S, respectively), the puckering amplitudes of each form (τ_N and τ_S, respectively), and the percent S form. This treatment required firm stereochemical assignments of the signals of the diastereotopic protons at C2 (H2*R*, H2*S*) and C4 (H4*R*, H4*S*) of **2**. The latter were assigned by using the "*syn*-upfield rule",[16] which was validated previously in aldotetrofuranosyl rings;[17] the more shielded C4 proton (defined as H4′) is *cis* to O3, and thus H4′ = H4*S* (Chart 3) (Table 1). However, application of this rule to assign the H2*R* and H2*S* signals is not possible due to the similarity in the interactions of these protons with O1 and O3. An inspection of $^3J_{HH}$ values involving H2′ (defined as the more shielded C2 proton) shows a moderately large coupling to H3 (5.9 Hz), whereas H2 (defined as the less shielded C2 proton) shows a considerably smaller coupling (1.8 Hz) to H3. We tentatively assigned H2′ = H2*S* (*cis* to H3) and H2 = H2*R* (*trans* to H3) (Table 1) (Chart 3) on the basis of these data. These assignments were then used in PSEUROT 6.2 calculations,[11a] yielding the following data: $P_N = -23.0°$; $P_S = 221.5°$; % S = 89%.[11b] Similar calculations using the reverse assignments for H2*R* and H2*S* gave unreasonable PSEUROT results (*e.g.*, root-mean-square deviations > 2

(12) (a) de Leeuw, F. A. A. M.; Altona, C. *J. Comp. Chem.* **1983**, *4*, 428−437. (b) Haasnoot, C. A. G.; de Leeuw, F. A. A. M.; de Leeuw, H. P. M.; Altona, C. *Org. Magn. Reson.* **1981**, *15*, 43−52.

(13) Frisch, M. J.; Trucks, G. W.; Head-Gordon, M.; Gill, P. M. W.; Wong, M. W.; Foresman, J. B.; Johnson, B. G.; Schlegel, H. B.; Robb, M. A.; Replogle, E. S.; Gomperts, R.; Andres, J. L.; Raghavachari, K.; Binkley, J. S.; Gonzales, C.; Martin, R. L.; Fox, D. J.; DeFrees, D. J.; Baker, J.; Stewart, J. J. P.; Pople, J. A. Gaussian 92, Revision C.3; Gaussian, Inc.: Pittsburgh, PA, 1992.

(14) (a) Serianni, A. S.; Chipman, D. M. *J. Am. Chem. Soc.* **1987**, *109*, 5297. (b) Serianni, A. S.; Wu, J.; Carmichael, I. *J. Am. Chem. Soc.* **1995**, *117*, 8645-8650. (c) Garrett, E. C.; Serianni, A. S. In *Computer Modeling of Carbohydrate Molecules*; French, A. D., Brady, J. W., Eds.; ACS Symp. Ser. 430; American Chemical Society: Washington, DC, 1990; pp 91−119. (d) Garrett, E. C.; Serianni, A. S. *Carbohydr. Res.* **1990**, *206*, 183−191.

(15) (a) Lemieux, R. U. *Pure Appl. Chem.* **1971**, *25*, 527−548. (b) Lemieux, R. U.; Koto, S.; Voisin, D. In *Anomeric Effect: Origin and Consequences*; Szarek, W. A., Horton, D., Eds.; ACS Symp. Ser. 87; American Chemical Society: Washington, DC, 1979; pp 17−29.

(16) Anteunis, M.; Danneels, D. *Org. Magn. Reson.* **1975**, *7*, 345.

(17) Serianni, A. S.; Barker, R. *J. Org. Chem.* **1984**, *49*, 3292−3300.

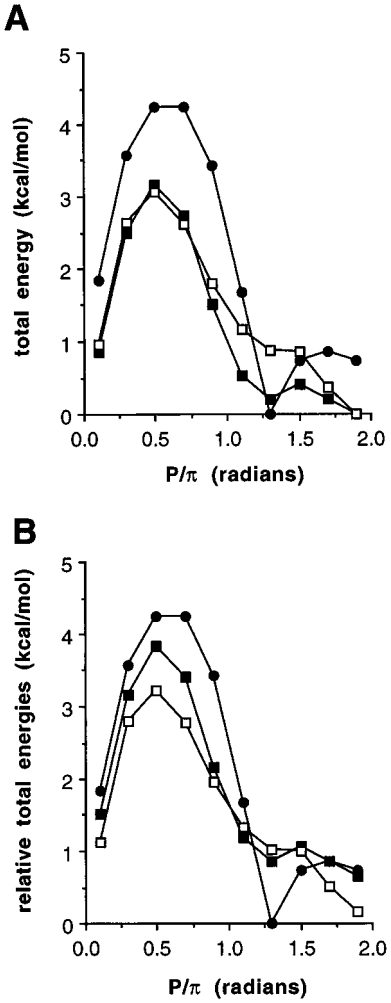

Figure 2. Effect of the C3−O3 torsion angle (Chart 1) on the conformational energy curve for **2** obtained from *ab initio* molecular orbital calculations (HF/6-31G*). (A) Total energy curves derived from individual data sets. (B) *Relative* total energy curves derived from the three data sets. Solid circles, Rotamer 2; open squares, Rotamer 3; solid squares, Rotamer 4.

Hz), thus providing indirect support for the assignments. The puckering amplitudes of the N and S forms were held constant at 38° in these calculations, since calculations in which these parameters were allowed to vary independently led to higher root-mean-square deviations and were therefore considered less reliable. The PSEUROT analysis indicates that S forms of **2** are more preferred (∼89%) than N forms (∼11%) in aqueous (^2H_2O) solution; the best fit yielded an S form near $^4T_3$ and an N form near E_2 (Figure 1).

Structure **2** was then subjected to molecular orbital calculations (HF/6-31G*) by using the initial C1−O1 and C3−O3 torsions shown in Chart 1. Three conformational energy curves were obtained by using data for the ten envelope (E) forms of **2** (Figure 2A) which differ only in the initial C3−O3 torsion angle used in the calculation. Energy minima occur at E_2 (N form) and ^4E (S form) in the three curves, but the *relative* energies of these two conformers depend on the C3−O3 torsion angle (see below). Importantly, the preferred N and S conformations of **2** derived via computation and NMR are similar; the NMR-derived N form (E_2) is identical with the computed N form, and the NMR-derived S form ($^4T_3$) is similar to the computed S form (^4E) (Figure 1). While the computations were restricted to E forms, the actual energy minima derived via MO calculations may occur at adjacent T forms when the partial planarity constraints are released, as found previously in other furanoses.[14a] This expectation was confirmed by releasing the

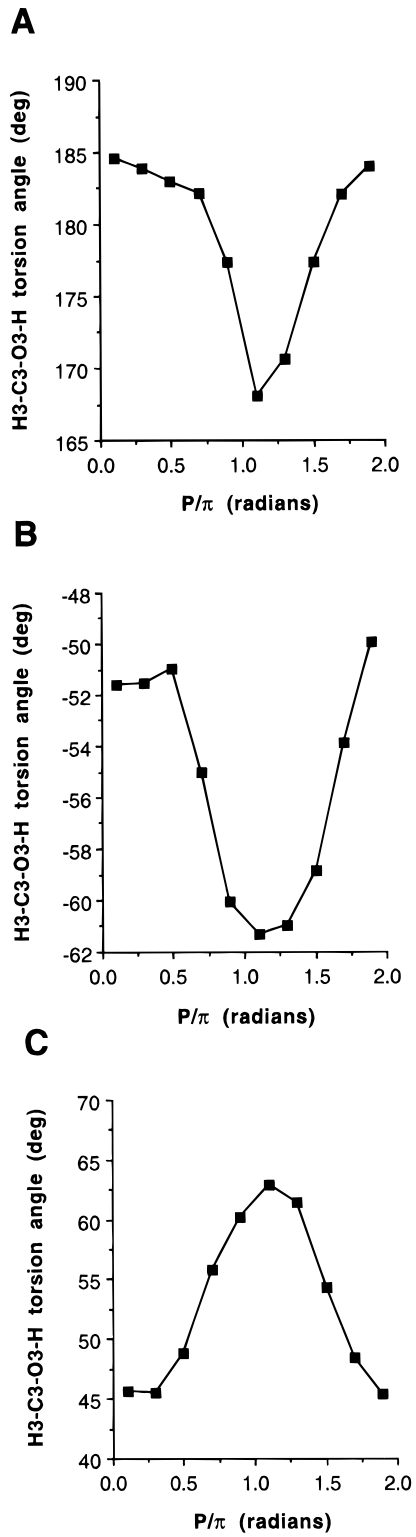

Figure 3. Effect of ring conformation on the optimized C3−O3 torsion angle in **2** (Chart 1): (A) Rotamer 2, (B) Rotamer 3, and (C) Rotamer 4.

O4−C1−C2−C3 and C3−C4−O4−C1 torsion angle constraints (fixed at 0°) in the ^4E and E_2 conformers of **2** (Rotamer 2), respectively. The restrained conformers gave P/τ_m values of 236°/43° and 341°/38°, respectively. The fully relaxed structures yielded P/τ_m values of 240°/40° and 331°/37°, respectively, indicating that the true energy minima occur at adjacent T forms. The energy lowering upon release of the final torsional constraint was <0.04 kcal/mol.

The data in Figure 2A indicate that *nonanomeric* C−O bond rotation in furanoses can significantly affect the *relative* energies of conformers;[14c] for example, in the present case rotation of

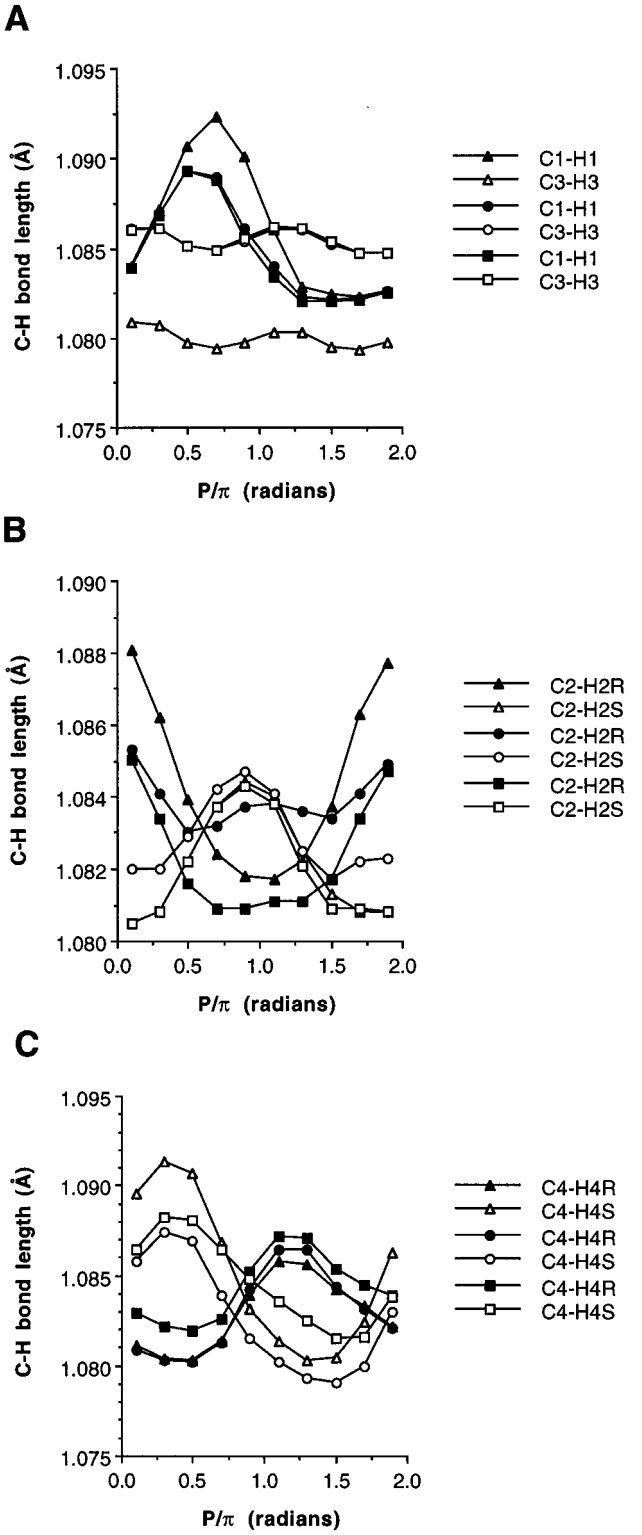

Figure 4. Effect of ring conformation on C−H bond lengths in **2** as a function of the C3−O3 torsion angle (triangles, Rotamer 2; circles, Rotamer 3; squares, Rotamer 4): (A) C1−H1 and C3−H3 bonds; (B) C2−H2*R* and C2−H2*S* bonds; and (C) C4−H4*R* and C4−H4*S* bonds.

the C3−O3 bond from Rotamer 2 to Rotamer 3 or 4 (Chart 1) shifts the global energy minimum from ^{4}E to E_2 (Figure 2A). In solution, the C3−O3 bond is expected to rotate relatively freely, thus potentially modulating the position of the global energy minimum. These results suggest that access to the N and S conformational minima of **2** requires *concerted endocyclic and exocyclic torsion angle change*, as suggested earlier.[14c] It should also be noted that, while the *locations* of the energy minima derived from the NMR and computational data are similar (see above), the strong preference for S forms (∼89%)

Chart 4

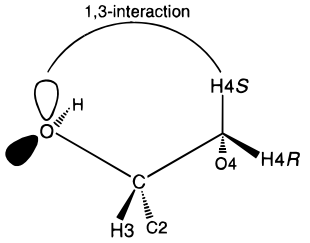

1,3-interaction between an O3 lone-pair orbital and the C4-H4*S* bond in the E_3 conformation (Rotamer 2)

indicated by $^3J_{HH}$ analysis is not consistent with the computational results. The global minimum of the three data sets occurs at ^{4}E (S form) of Rotamer 2, whereas the next most stable conformer is E_2 (N form) of Rotamer 3 (Figure 2B); the energy difference, 0.16 kcal/mol, indicates a proportion of S forms (∼57%) smaller than determined by NMR. While the error associated with the computed energy difference may account for some of this discrepancy, these results suggest the potential involvement of solvation in stabilizing or destabilizing specific furanose conformers in solution. In a similar vein, the application of the PSEUROT method to the analysis of $^3J_{HH}$ values assumes a two-state exchange process between N and S conformers separated by a relatively high energy barrier, such that the intermediate conformers along the interconversion pathway do not contribute to the observed couplings. However, the barrier height for N/S exchange in **2**, as determined by *ab initio* MO calculations (Figure 2), is <1 kcal/mol. Thus, the observed agreement between solution and computed forms of **2**, while possibly coincidental, may indicate the involvement of solvent water in preferentially stabilizing the N/S conformers, thereby enhancing the energy barrier between them. Nevertheless, given the limitations of the PSEUROT treatment of $^3J_{HH}$ values, the modest computational method and basis set used in the calculations, and the neglect of solvation effects inherent to the *ab initio* method applied here, the degree of consistency between theory and experiment is reassuring, thus justifying a computational analysis of the protonated form of **2** (*i.e.*, **1**).

B. Effect of the C3−O3 Torsion Angle on the Structure of 2. As noted above, the conformational energy profile for **2** depends on the C3−O3 torsion angle (Figure 2A,B). The optimized C3−O3 torsion varied systematically with ring conformation in each of the three sets of calculations (Figure 3).

A number of structural parameters in **2** are affected by the C3−O3 torsion angle. The length of C−H bonds *cis* to the C3−O3 bond (*i.e.*, C1−H1, C2−H2*R*, C4−H4*S*) is, in general, more affected by the C3−O3 torsion angle than the length of C−H bonds *trans* to the C3−O3 bond (Figure 4A−C). For example, the C4−H4*R* bond is essentially unaffected by the C3−O3 torsion angle (Figure 4C), whereas substantial effects are observed for the C4−H4*S* bond (Figure 4C). These effects may be explained by invoking a 1,3-effect of an oxygen lone-pair orbital on C−H bond lengths (Chart 4); the presence of this 1,3-interaction *reduces* the C−H bond length. This 1,3-effect, superimposed on the C−H bond orientation and vicinal lone-pair effects on C−H bond lengths discussed previously,[14b,18] provides an internally consistent qualitative explanation of the C−H bond length behaviors shown in Figure 4. For example, the C4−H4*R* bond experiences the same interactions with a lone-pair orbital on O3 throughout the pseudorotational itinerary for Rotamers 2 and 3; thus, in ^{3}E, a 1,3-interaction is present for both C3−O3 rotamers whereas it is absent in E_3. Conse-

(18) Podlasek, C. A.; Stripe, W. A.; Carmichael, I.; Shang, M.; Basu, B.; Serianni, A. S. *J. Am. Chem. Soc.* **1996**, *118*, 1413−1425.

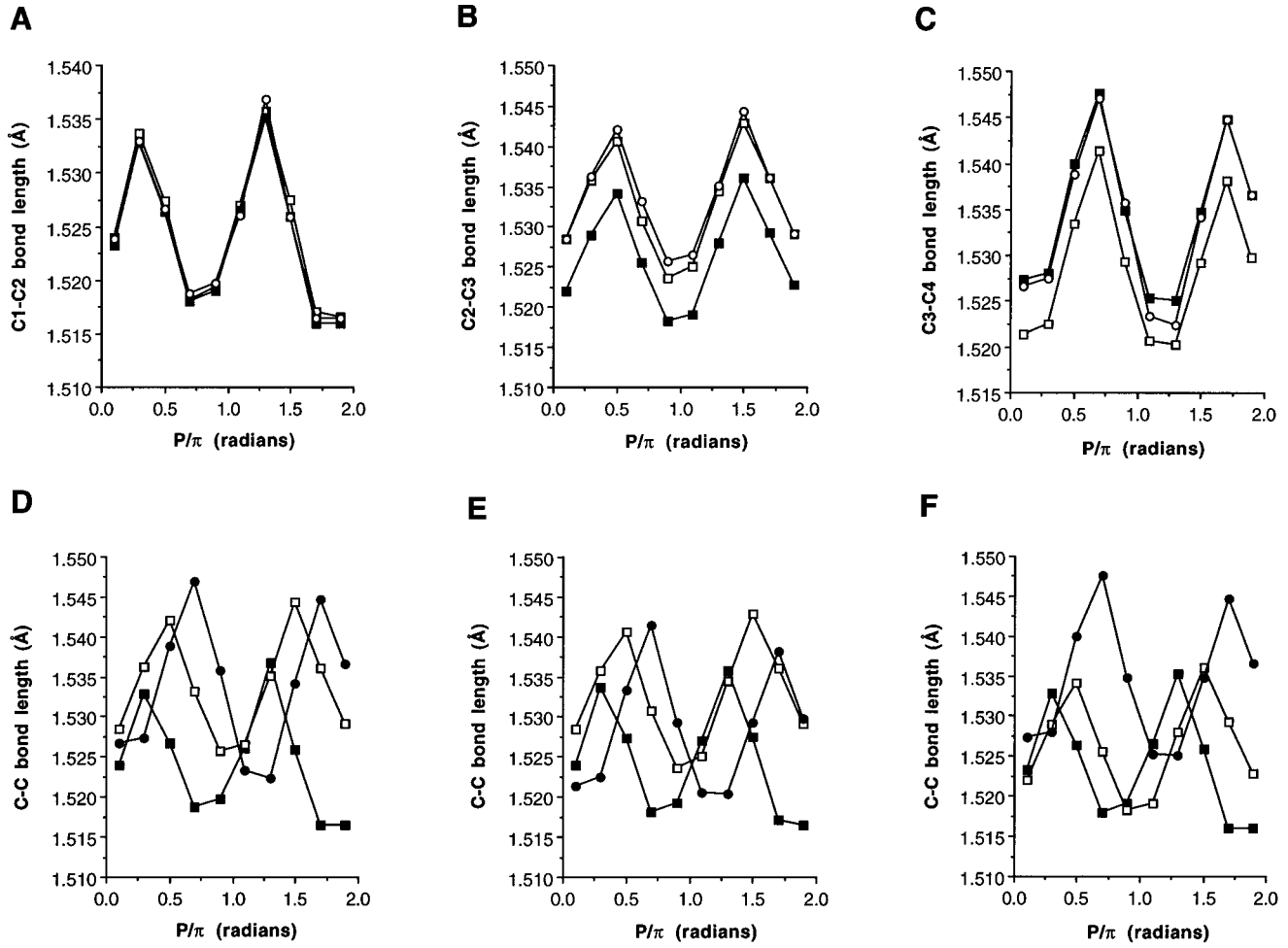

Figure 5. Effect of ring conformation on C−C bond lengths in **2** as a function of the C3−O3 torsion angle: (A) C1−C2 bond (open circles, rotamer 2; open squares, Rotamer 3; closed squares, Rotamer 4), (B) C2−C3 bond (open circles, Rotamer 2; open squares, Rotamer 3; closed squares, Rotamer 4), and (C) C3−C4 bond (open circles, Rotamer 2; open squares, Rotamer 3; closed squares, Rotamer 4), (D) behavior of the three C−C bonds in Rotamer 2 (solid squares, C1−C2; open squares, C2−C3; closed circles, C3−C4), (E) behavior of the three C−C bonds in Rotamer 3 (solid squares, C1−C2; open squares, C2−C3; closed circles, C3−C4), and (F) behavior of the three C−C bonds in Rotamer 4 (solid squares, C1−C2; open squares, C2−C3; closed circles, C3−C4).

quently, both curves are similar (Figure 4C). On the other hand, a larger decrease in the C4−H4*S* bond length is observed in N forms relative to S forms for Rotamer 3; in N forms (*e.g.*, ^{3}E), a 1,3-interaction is present for Rotamer 3 but not for Rotamer 2, whereas C4−H4*S* experiences 1,3-interactions for both Rotamers 2 and 3 in S forms (*e.g.*, E_3) (Figure 4C). A similar effect is observed for C2−H2*S*, which is shorter in N forms for Rotamers 2 and 4 (Figure 4B); in N forms, a 1,3-interaction is present for Rotamers 2 and 4 but not for Rotamer 3. In S forms, the C2−H2*S* bond experiences no 1,3-interactions with O3 in any of the C3−O3 rotamers, and thus bond lengths are similar (Figure 4B). The C2−H2*R* bond length for Rotamer 2 exceeds that for Rotamer 3 in N forms, whereas the opposite is observed in S forms (Figure 4B). This behavior is caused by the presence of 1,3-interactions in N forms for Rotamer 3 which are absent in N forms for Rotamer 2, and the presence of 1,3-interactions in S forms for Rotamer 2 which are absent in S forms for Rotamer 3.

The above 1,3-lone-pair orbital effects are superimposed on *vicinal* O4 lone-pair interactions for the C4−H4*R* and C4−H4*S* bonds (*anti* orientations cause bond elongation),[14a−c,18] and the effect of C−H bond orientation on length (quasiequatorial bonds are shorter than quasiaxial bonds)[14a−c,18] for the C2−H2*R*, C2−H2*S*, C4−H4*R*, and C4−H4*S* bonds. Thus, for example, the shortening of the C2−H2*R* bond in S forms (quasiequatorial orientation) is *enhanced* for Rotamer 2 relative to Rotamer 3 due to the presence of a 1,3-interaction with an O3 lone-pair orbital, and the same bond, when quasiaxial (*i.e.*, in N forms), is maximal in length due to orientational effects and the *absence* of 1,3-lone-pair interactions. In contrast, for Rotamer 3, the C2−H2*R* bond experiences a 1,3-interaction in N forms which *opposes* the orientational lengthening effect (quasiaxial orientation), whereas in S forms, no 1,3-interaction is present to enhance the bond shortening caused by orientation (bond is quasiequatorial). Consequently, the *overall* change in length of the C2−H2R bond (Rotamer 3) with ring conformation is considerably smaller than that observed for the C2−H2*R* bond (Rotamer 2) (Figure 4B).

The dependence of the C3−H3 bond length on ring conformation is similar for Rotamers 2−4, but the curve is displaced to longer lengths for Rotamers 3 and 4 (Figure 4A). The latter lengthening is attributed to vicinal O3 lone-pair effects on the C3−H3 bond lengths;[14b,18] in Rotamers 3 and 4, the lone pair antiperiplanar to the C3−H3 bond (Chart 1) increases the bond length. This arrangement is absent for Rotamer 2. The "vicinal lone-pair effect" also explains, in part, the observed dependence of the C1−H1, C4−H4*R*, and C4−H4*S* bond lengths on ring conformation, as discussed previously.[14b,18]

The C1−C2, C2−C3, and C3−C4 bond lengths in **2** depend on ring conformation and on the C3−O3 torsion angle (Figure 5). Two maxima and two minima are observed for each C−C bond, with maxima occurring in conformations having the out-of-plane ring atom opposite to the C−C bond (*e.g.*, the C2−C3 bond shows maximal lengths in the ^{o}E and E_o conformations;

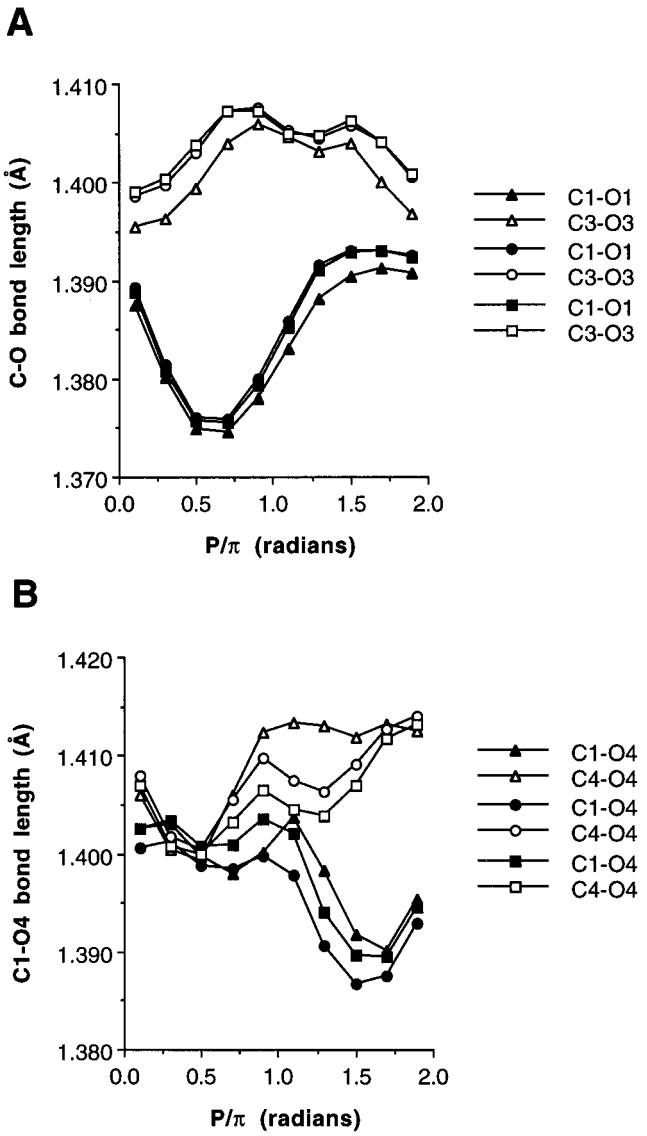

Figure 6. Effect of ring conformation on exocyclic (A) and endocyclic (B) C−O bond lengths in **2** as a function of the C3−O3 torsion angle (triangles, Rotamer 2; circles, Rotamer 3; squares, Rotamer 4).

Figure 5B), and minima occurring in conformations having either carbon in the C−C bond out-of-plane (*e.g.*, $^2E/E_3$ and $E_2/^3E$ for the C2−C3 bond; Figure 5B). In **2**, the C1−C2 bond length is unaffected by the C3−O3 torsion angle (Figure 5A), whereas the C2−C3 and C3−C4 bond lengths are sensitive to this torsion (Figure 5B,C). These results are consistent with the vicinal lone-pair effect discussed above in the context of C−H bond lengths. The longer C2−C3 bond in Rotamers 2 and 3 relative to that in Rotamer 4 (Figure 5B) in all ring conformations is caused by the presence of a vicinal interaction with an O3 lone-pair orbital. The longer C3−C4 bond in Rotamers 2 and 4 relative to that in Rotamer 3 (Figure 5C) can be explained in a similar fashion. The *relative* C−C bond lengths in **2** also depend on the C3−O3 torsion angle (Figure 5D−F); although not investigated here, the C1−O1 torsion angle is expected to exert similar effects on the C1−C2 bond length. Likewise, bond-lengthening effects on the C1−C2 and C3−C4 bonds might be anticipated by O4 lone-pair orbitals in the ^oE and E_o conformations, although this effect appears small.

Exocyclic C−O bond lengths (C1−O1, C3−O3) are slightly affected by C3−O3 bond torsion; these bonds are slightly shorter in Rotamer 2 (Figure 6A). These bonds are longer when quasiaxial and shorter when quasiequatorial as discussed

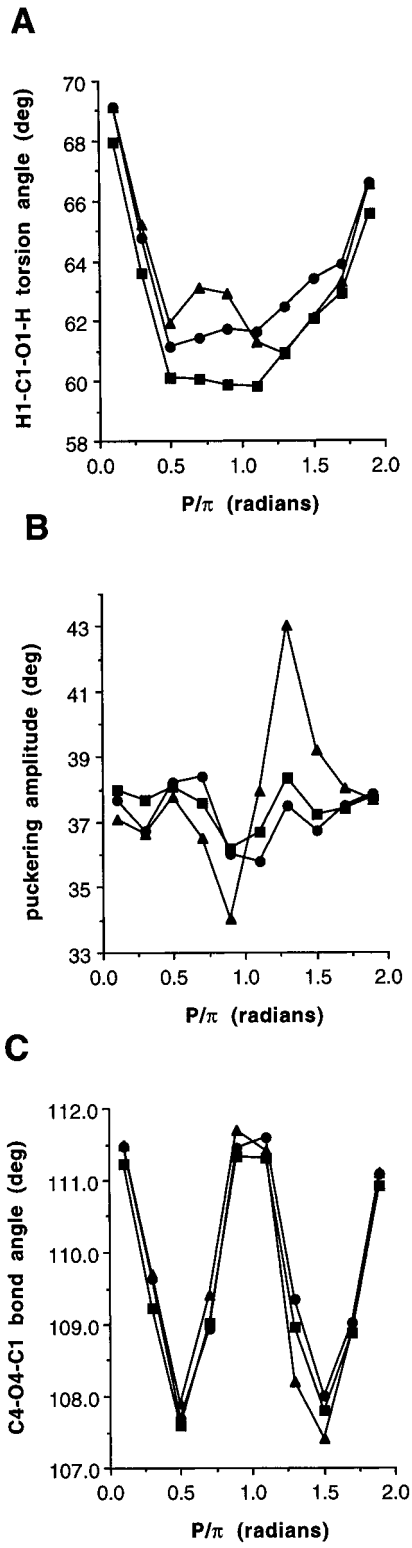

Figure 7. Effect of ring conformation on the H1−C1−O1−H torsion angle (A), puckering amplitudes[19] (τ_m) (B), and the C4−O4−C1 bond angle (C) in **2** as a function of C3−O3 torsion angle (triangles, Rotamer 2; circles, Rotamer 3; squares, Rotamer 4).

previously,[14b,18] although the trend is more clearly observed for the C1−O1 bond. The endocyclic C−O bonds (C1−O4, C4−O4) appear to be more affected by the C3−O3 torsion angle in west conformers ($P/\pi = 1-2$) (Figure 6B). The shortening of the C4−O4 bond observed in Rotamers 3 and 4 relative to Rotamer 2 in west forms may be attributed to the 1,3-lone-pair effect (involving O3) described above. The shortening of the C4−O4 bond caused by this effect may in turn induce the slight contraction of the C1−O4 bond observed in Rotamers 3 and 4

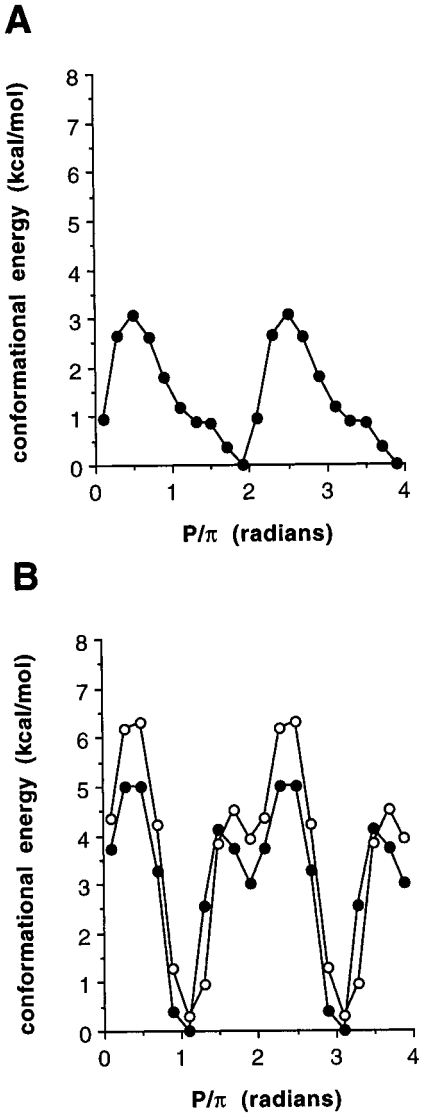

Figure 8. (A) Conformational energy curve for **2** (Rotamer 3). (B) Conformational energy curves for the two protonated forms of **1** (closed circles, molecule A; open circles, molecule B).

relative to Rotamer 2. The large decrease in the C1−O4 bond length in west conformers (Figure 6B) is caused by n → σ^* donation by an O4 lone pair when antiperiplanar to the C1−O1 bond.

The exoanomeric torsion angle, H1−C1−O1−H, in **2** is affected by ring conformation and the exocyclic C3−O3 torsion angle, and appears minimal in S forms (60−63°) and maximal in N forms (65−69°) (Figure 7A). The effect of ring conformation on puckering amplitude (τ_m) is essentially the same for Rotamers 3 and 4 (Figure 7B), but significant differences are observed for the ^{2}E (less puckered) and ^{4}E (more puckered) forms in Rotamer 2.[19] This latter behavior may be caused by repulsive interactions in the ^{2}E conformer (between O3−H and the axial H1) and attractive interactions in the ^{4}E conformer

(19) Puckering amplitudes (τ_m) reported in Figures 7B and 14D were computed by using the five ring torsion angles (τ_0(C4−O4−C1−C2), τ_1(O4−C1−C2−C3), τ_2(C1−C2−C3−C4), τ_3(C2−C3−C4−O4), τ_4(C3−C4−O4−C1)) and the following equation, tan $P = [(\tau_4 + \tau_1) - (\tau_3 + \tau_0)]/[2\tau_2(\sin 36° + \sin 72°)]$, to first compute the pseudorotation phase angle, P, for each E form. The value of P was then used to compute τ_m by using the following equation, $\tau_j = \tau_m \cos[P + 0.8\pi(j - 2)]$, where $j = 0-4$ (for each of the five τ values above) and $\pi = 180°$. This procedure to derive P and τ_m values from τ_0 to τ_4 is discussed in ref 11a and the following reference: Olson, W. K.; Sussman, J. L. *J. Am. Chem. Soc.* **1982**, *104*, 270−278. Figure 7B shows τ_m values computed in this fashion for Rotamers 2−4 of **2**; average values of 37−38° are observed, in good agreement with the 38° values used in the PSEUROT analysis of **2**.

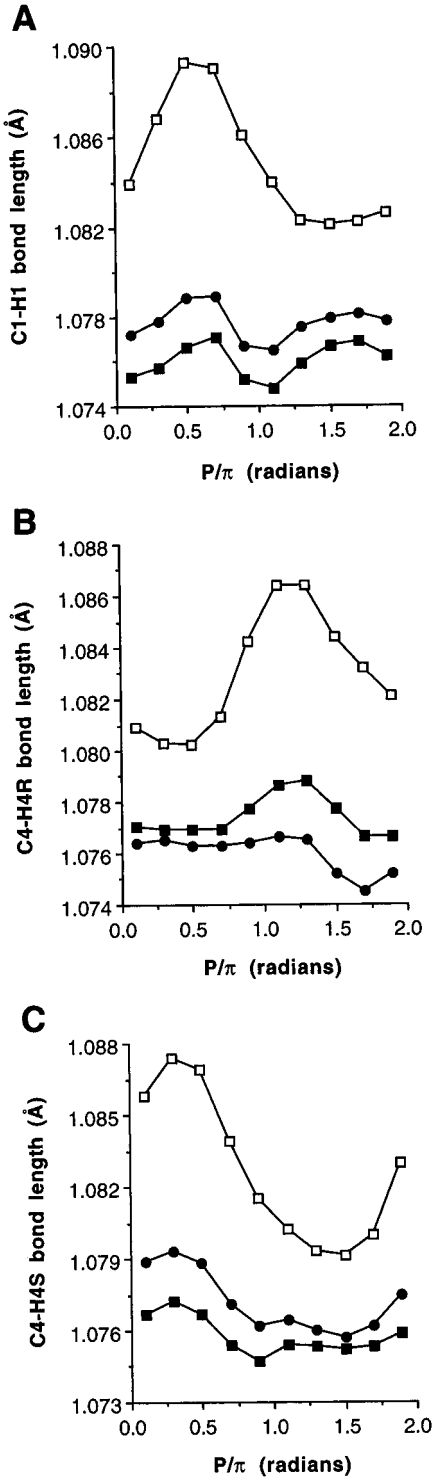

Figure 9. Effect of O4 protonation on C−H bond lengths in **2** involving C1 and C4: (A) C1−H1, (B) C4−H4*R*, and (C) C4−H4*S*. Open squares, unprotonated **2**; closed squares, molecule A; closed circles, molecule B.

(between O3−H and an O4 lone-pair orbital). It should be noted that the average computed τ_m value for Rotamers 2−4 is 37−38°, thus providing justification for restraining the τ_m values to 38° in the PSEUROT calculations on **2** (see above). The C4−O4−C1 bond angle is maximal in E_2/^{3}E and ^{2}E/E_3 forms, and minimal in ^{o}E and E_o forms (Figure 7C), and very little dependence on the C3−O3 torsion angle is observed.

C. Effect of O4 Protonation on the Structure of 2. Ring-oxygen (O4) protonation of **2** gives two stable forms of **1**, designated molecules A and B (Chart 2). This protonation results in major changes in the conformational preferences of

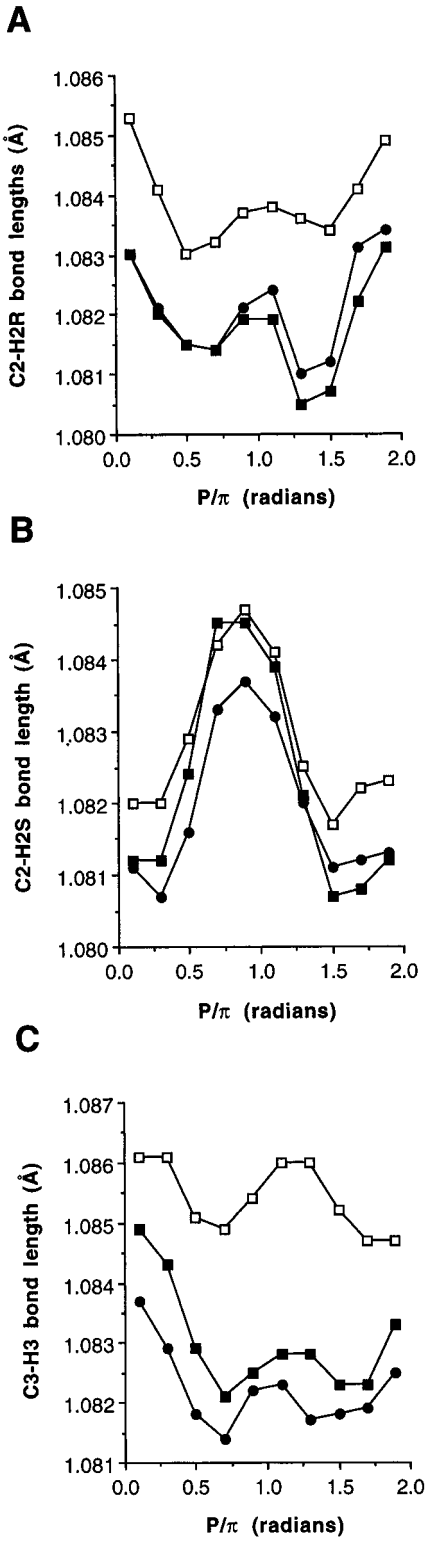

Figure 10. Effect of O4 protonation on C−H bond lengths in **2** involving C2 and C3: (A) C2−H2*R*, (B) C2−H2*S*, and (C) C3−H3. Open squares, unprotonated **2**; closed squares, molecule A; closed circles, molecule B.

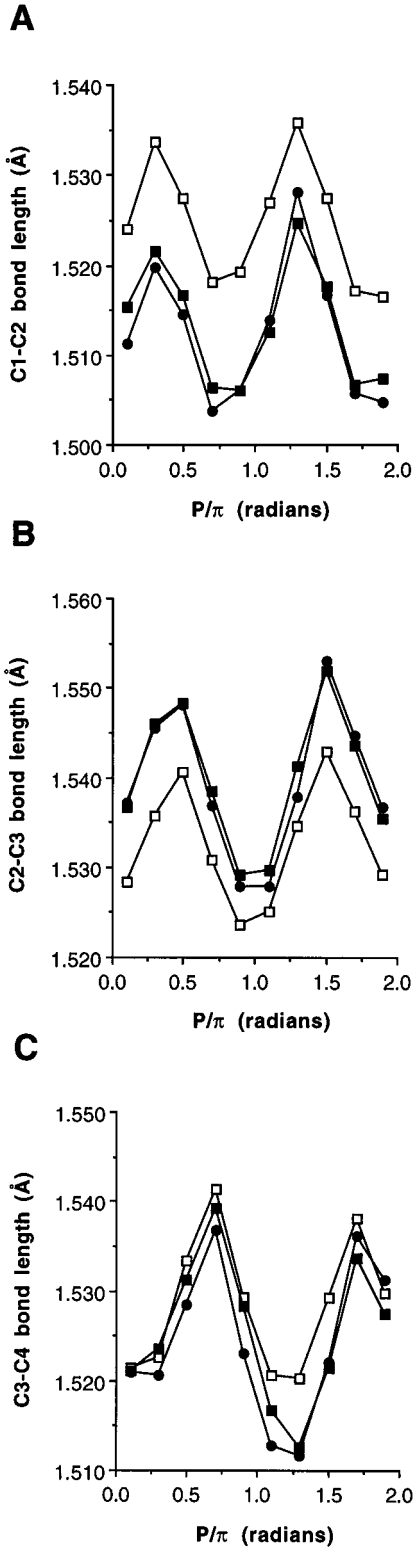

Figure 11. Effect of O4 protonation on C−C bond lengths in **2**: (A) C1−C2, (B) C2−C3, and (C) C3−C4. Open squares, unprotonated **2**; closed squares, molecule A; closed circles, molecule B.

the furanose ring (Figure 8). The minimum energy conformation of **2** (Rotamers 1 and 3; Chart 1) is E_2 (Figures 2 and 8A), with a local minimum located near ^4E. O4 Protonation shifts the global energy minimum to E_3 and the local minimum to E_2 in molecules A and B (Figure 8B). The barriers for N/S interconversion are substantially higher for **1** than for **2**; barrier heights are lower for interconversion via west forms than via east forms for both **1** and **2** (Figure 8A,B). Thus, O4 protonation of **2** changes the preferred ring conformation (E_2 to E_3) and significantly *decreases* the conformational flexibility of the ring, although the preferred pathway for N/S interconversion appears to be conserved in **1** and **2**.

Major structural changes are also observed when **2** is converted to **1**. The C1−H1, C4−H4*R*, and C4−H4*S* bond lengths decrease substantially in the protonated form (Figure 9). In addition, ring-oxygen protonation reduces the sensitivity of these bond lengths to changes in ring conformation. Smaller decreases are observed in the C2−H2*R*, C2−H2*S*, and C3−H3 bond lengths upon O4 protonation (Figure 10). The C1−C2 and C3−C4 bond lengths decrease upon protonation, more

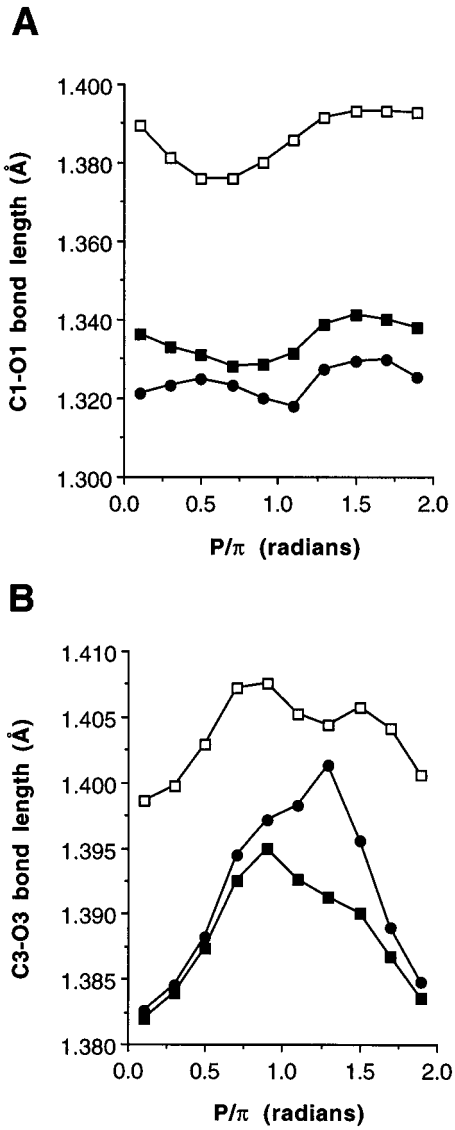

Figure 12. Effect of O4 protonation on exocyclic C−O bond lengths in **2**: (A) C1−O1 and (B) C3−O3. Open squares, unprotonated **2**; closed squares, molecule A; closed circles, molecule B.

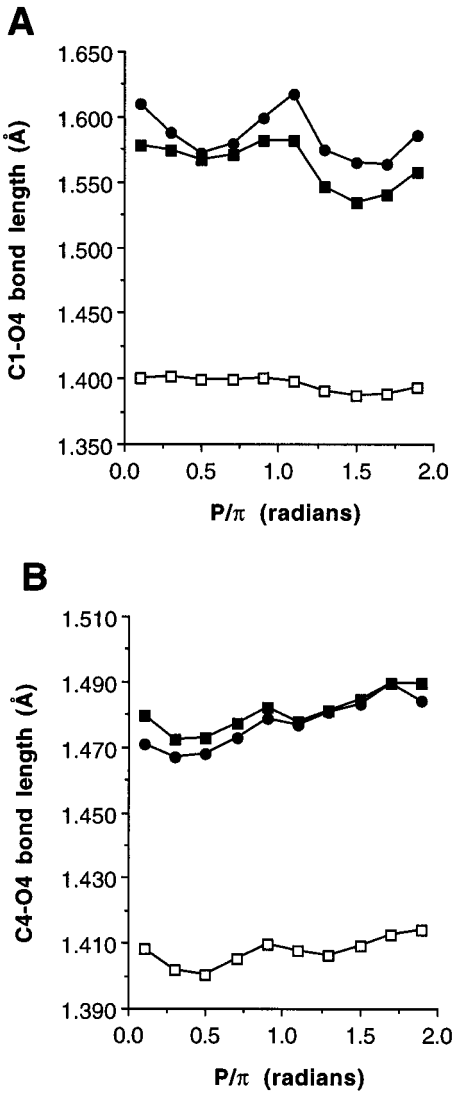

Figure 13. Effect of O4 protonation on endocyclic C−O bond lengths in **2**: (A) C1−O4 and (B) C4−O4. Open squares, unprotonated **2**; closed squares, molecule A; closed circles, molecule B.

notably for C1−C2 (Figure 11A,C); in contrast, the C2−C3 bond length increases slightly in the protonated forms (Figure 11B). The C1−O1 bond length decreases significantly (>0.05 Å) (Figure 12A), whereas a more modest decrease is observed in the C3−O3 bond length (Figure 12B). The endocyclic C−O bonds (C1−O4, C4−O4) increase in length upon protonation; the C1−O4 and C4−O4 bonds increase by ∼0.2 and ∼0.06 Å, respectively (Figure 13). These C−O bond length changes are similar to those observed in previous investigations of protonated methanediol[20a,b] and dimethoxymethane,[20c] and protonated 2-methoxytetrahydropyrans.[21]

The C4−O4−C1 bond angle shows the same general dependence on ring conformation in **1** and **2** (Figure 14A), although the position of protonation appears to affect this angle (*e.g.*, the angle is significantly different in E_o of molecule A and B). Optimized H1−C1−O1−H and H3−C3−O3−H torsion angles differ in **1** and **2**, with both angles smaller (absolute value) in the protonated forms (Figure 14B,C). Puckering amplitude (τ_m) is relatively constant throughout the pseudorotational itinerary for **2** (Rotamer 3), whereas more defined τ_m minima are observed at the $E_4/^oE$ and/or $E_3/^4E$ conformations of **1** (Figure 14D). The O4−H bond length in **1** is minimal near $P/\pi = 0.9$ (^2E) and 1.9 (E_2), and maximal near $P/\pi = 0.5$ (^oE) and 1.5 (E_o) (Figure 15A). The dependence of the C2−C1−O4−H torsion angle on ring conformation differs in the two protonated forms of **1**, as expected (Figure 15B,C).

D. Implications of the Structural Changes Induced by O4 Protonation. The above results show that protonation at O4 of **2** causes substantial structural changes in the furanose ring. The largest changes in bond lengths occur for bonds in the vicinity of O4. For example, the C1−O4 and C4−O4 bond lengths increase by ∼14% and ∼5%, respectively, in the E_3 conformer, and the C1−O1 bond decreases by ∼4% (Figure 16). All remaining bonds in **2** except C2−C3 decrease in length upon protonation (0.02−0.94%); a ∼0.3% increase is observed in the C2−C3 bond length (Figure 16). These structural changes have important mechanistic implications for the acid-catalyzed anomerization of **2**, which is believed to involve O4 protonation (Scheme 1). Structural changes induced by ring-oxygen protonation generate an intermediate **1** that is predisposed toward ring-opening due to the elongated C1−O4 bond (which breaks in the ring-opening event) and the shorter C1−O1 and C1−H1 bonds (which contract in the acyclic aldehyde form). Thus,

(20) (a) Wipff, G. *Tetrahedron Lett.* **1978**, *35*, 3269−3270. (b) Woods, R. J.; Szarek, W. A.; Smith, V. H., Jr. *J. Chem. Soc., Chem. Commun.* **1991**, *5*, 334−33. (c) Andrews, C. W.; Bowen, J. P.; Fraser-Reid, B. *J. Chem. Soc., Chem. Commun.* **1989**, *24*, 1913−1916.

(21) Andrews, C. W.; Fraser-Reid, B.; Bowen, J. P. *J. Am. Chem. Soc.* **1991**, *113*, 8293−8298.

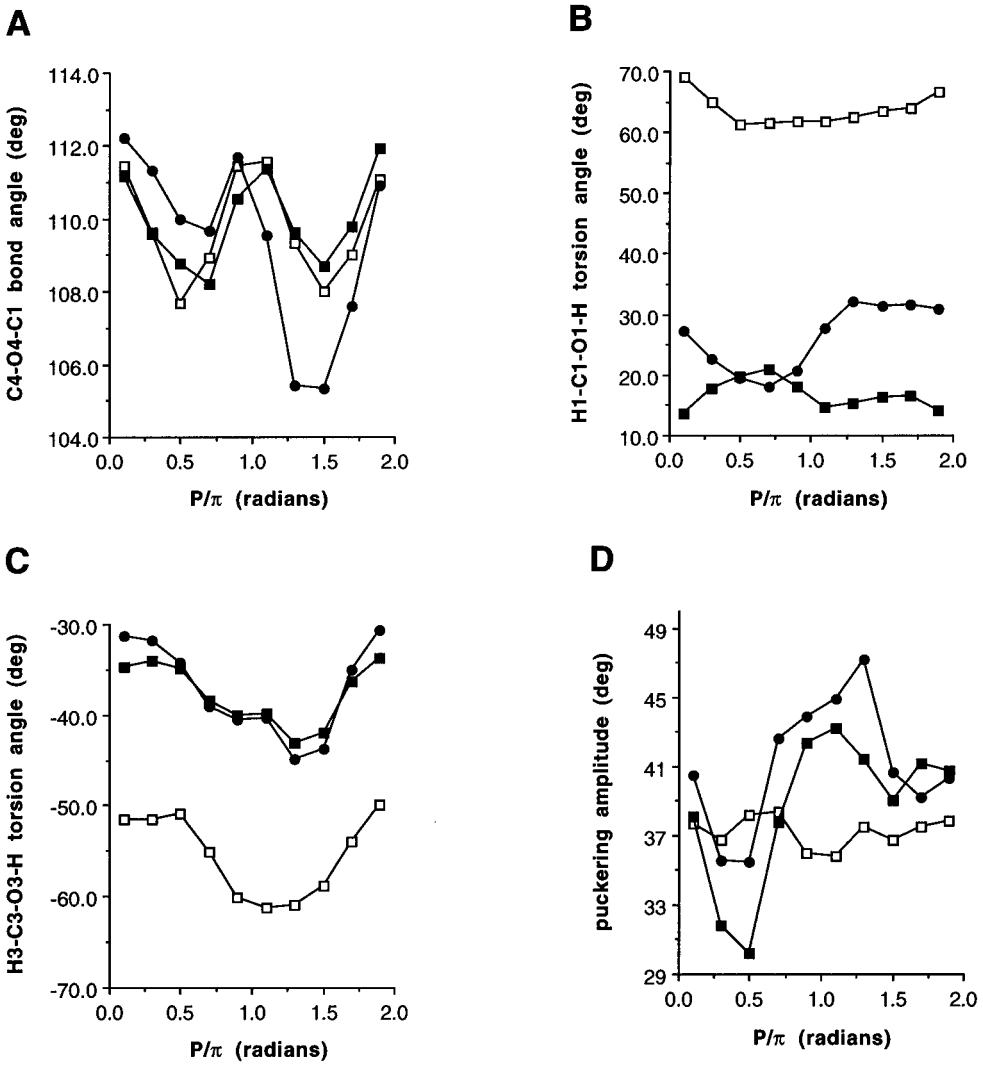

Figure 14. Effect of O4 protonation on several structural parameters in **2**: (A) C4−O4−C1 bond angle, (B) H1−C1−O1−H torsion angle, (C) H3−C3−O3−H torsion angle, and (D) puckering amplitudes (τ_m). Open squares, unprotonated **2**; closed squares, molecule A; closed circles, molecule B.

hydrogen ion, supplied either by an acid in solution or by a residue in an enzyme-active site, enhances ring-opening by *inducing structural changes in the furanose ring that move the reactant closer to the transition state*. The effect of O4 protonation is not structurally localized but pervasive (see, for example, Figure 16). Catalysis by hydrogen ion is not adequately "explained" as simply generating an "electron sink" at O4 to which electrons flow, as commonly viewed (Scheme 1). Protonation induces extensive structural changes in the furanose ring that produce an intermediate more closely resembling the transition state of the reaction than the initial reactant.

The protonation of O4 also induces a major change in the conformational behavior of **2**. This change is not unexpected, given that it must be mediated by the above-noted structural effects. A preferred N/S mixture for **2** involving the E_2 and ^4E forms shifts to a highly preferred S form (E_3) in both protonated forms of **1**. In addition, *the conformational rigidity of the molecule increases in the protonated state*, as indicated by the larger energy barriers for pseudorotation in **1** relative to **2**. This enhanced rigidity may have implications for enzyme catalysis involving protonated structures similar to **1**. In addition to generating an intermediate that more closely resembles the transition state, protonation by an active site residue would reduce the conformational mobility of the bound substrate. This loss of conformational entropy, in addition to entropy loss that may occur upon initial binding of the substrate, may affect the efficiency of the enzyme catalyst, that is, subsequent chemical reactions may be facilitated on a bound protonated intermediate having a more rigid conformation.

Conclusions

Chemical and biochemical (enzymic) reactions of carbohydrates frequently involve protonation events which function to stimulate reactivity. While the involvement of protonated intermediates in these reactions is well accepted, the effects of protonation on carbohydrate structure and conformation are not well appreciated. These effects can be studied with the use of computational methods that permit an assessment of the molecular properties of transient reaction intermediates that cannot be examined easily by current experimental methods.

In this investigation, *ab initio* molecular orbital calculations (HF/6-31G*) were applied to assess the effect of ring-oxygen protonation on the structure and conformation of 2-deoxy-β-D-*glycero*-tetrofuranose **2**. We first attempted to validate the computational method by comparing the conformational properties of the unprotonated furanose **2** derived from an analysis of $^3J_{HH}$ spin-coupling constants with those predicted from the calculations. The good agreement observed between theory and experiment for **2** leads to the reasonable expectation that the structural and conformational data computed for **1** are reliable. It should be appreciated, however, that the present study applies

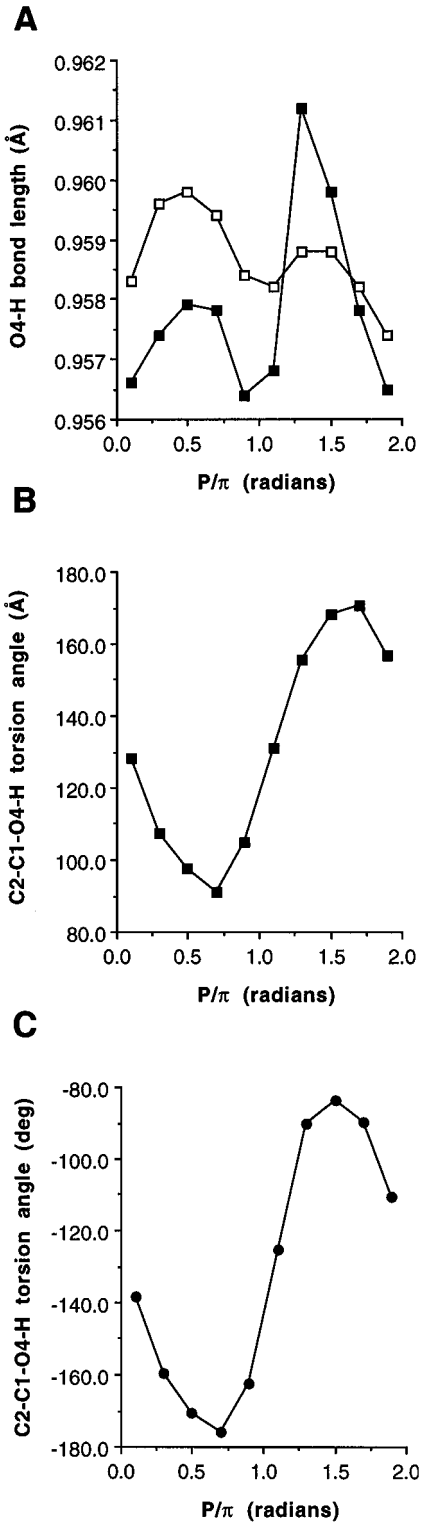

Figure 15. (A) Effect of ring conformation on the O4−H bond length in molecule A (open squares) and molecule B (closed squares). (B) Effect of ring conformation on the C2−C1−O4−H torsion angle for molecule A. (C) Effect of ring conformation on the C2−C1−O4−H torsion angle for molecule B.

a level of theory (HF/6-31G*) that does not take electron correlation effects into account, and the neglect of the latter in *ab initio* calculations on carbohydrates is known to lead to an overestimation of relative conformational energies[14b] and possibly to other deviations. Thus, while the data presented in this report cannot be considered quantitative, they are considered reliable with respect to predicting *overall trends* in a given molecular parameter, which is sufficient given the aims of the present work.

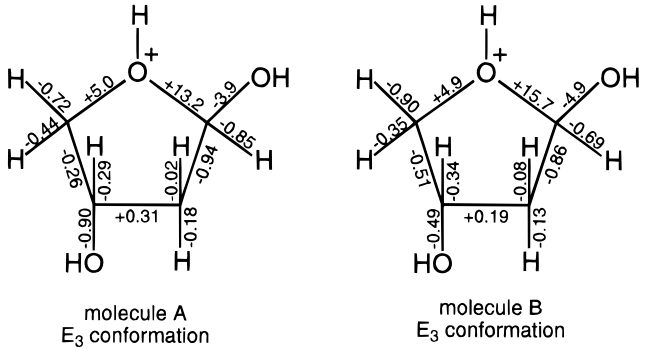

Figure 16. Percent changes in bond lengths in the E_3 conformation upon O4 protonation of **2** (Rotamer 3) to give molecule A (left) and molecule B (right).

The protonation of O4 of **2** produces two stable products (molecules A and B; Chart 2) that differ in the orientation of the proton about O4. *Ab initio* molecular orbital data on these two forms are similar but not identical. Thus, if discrimination of the two forms were possible, different reactivities might be expected. However, given the small size of H^+, both protonated forms may interconvert in an enzyme active site, even though one lone-pair orbital on O4 might be closer to the proton donor than the other.

This study has shown that protonation of the ring oxygen of furanose rings induces substantial changes in ring structure and conformation. Interestingly, the C1−O4 and C4−O4 bond lengths increase significantly upon protonation, while the C1−O1 and C1−H1 bond lengths decrease. Thus, **1** assumes structural features more closely resembling the transition state in anomerization in which the C1−O4 bond is breaking, while the shortening of the C1−H1 and C1−O1 bonds indicates incipient sp^2 character at C1. These bond length changes are probably induced by a "reverse anomeric effect".[15a,22a,b] The $E_2/^4E$ conformational model for **2** in ^2H_2O solvent results in an *average* C1−O1 bond orientation that is quasiaxial or near quasiaxial. This preferred disposition is consistent with previous experimental and computational results,[17,18] indicating the presence of an "anomeric effect"[23] in furanose rings in aqueous solution.[17] Protonation at O4 shifts this preferred disposition toward a quasiequatorial orientation (E_3 conformer), which is consistent with a reverse effect induced by the presence of positive charge on O4. In addition, O4 protonation of **2** may be viewed as analogous to the protonation of H_2O. In the latter case, the product H_3O^+ assumes a pyramidal geometry; the H−O−H bond angle increases from ∼104° in H_2O to ∼110° in H_3O^+. The structural contraints imposed by the ring in **1** prevent the attainment of ideal pyramidal geometry about O4. However, energy maxima are observed at or near the E_o and ^oE conformers of **1**, that is, in geometries in which the C4−O4−O1 bond angle is minimal; in contrast, maximal or near maximal values of this angle are observed at the global energy minumum E_3 form. Likewise, ring puckering is minimal near E_o and ^oE forms, and near maximal near E_3.

Protonation of O4 of **2** reduces the conformational flexibility of the furanose ring, as indicated by the enhanced barriers of pseudorotation observed for **1** relative to **2**. This rigidity is partly related to conformational behavior observed in aldono-

(22) (a) Perrin, C. L.; Armstrong, K. B. *J. Am. Chem. Soc.* **1993**, *115*, 6825−6834. (b) Wolfe, S.; Whangbo, M.-H.; Mitchell, D. J. *Carbohydr. Res.* **1979**, *69*, 1.

(23) (a) Lemieux, R. U. In *Molecular Rearrangements*; de Mayo, P., Ed.; Wiley-Interscience: New York, 1963; p 713. (b) Juaristi, E.; Cuevas, G. *The Anomeric Effect*; CRC Press: Boca Raton, FL, 1995.

1,4-lactones **7**, where the presence of an sp^2-hydridized carbon

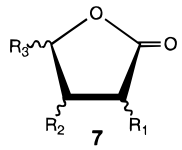

7

in the furanoid ring, and the accompanying planarity of the O4−C1(O1)−C2 fragment, reduces the conformational flexibility of the ring.[24] While the pseudorotational behavior of **1** is not as restricted as that of **7** (*i.e.*, the full range of E and T forms remains accessible to **1** but not to **7**), the ease with which some of the conformers can form is reduced significantly.

While the observed effects of O4 protonation lead to a more tangible explanation of the effect of acid catalysis on aldofuranose anomerization, it should be appreciated that the results reported in this investigation are, in the strictest sense, relevant to the unsolvated, gas-phase molecule. It remains to be established whether solvation, especially in aqueous solution, modulates the extent to which ring structure and conformation change as a consequence of O4 protonation. Furthermore, in a hypothetical enzyme-catalyzed reaction, the chemical environment of a furanose substrate will differ significantly from that in solution, with functional groups in the active site substituting for solvent molecules. This modified "solvation" may reinforce or oppose the structural and conformational effects reported here.

This investigation confirms previous reports identifying a dependence of C−H bond length in furanose rings on C−H bond orientation.[14b,18] In the absence of other factors, a given C−H bond is longer when quasiaxial than when quasiequatorial (the orientation factor). However, at least two additional factors appear to modulate this behavior: vicinal lone-pair effects and 1,3-lone-pair effects, the latter newly described in this report. These latter factors appear to have opposing effects on C−H bond lengths. The presence of a lone-pair orbital antiperiplanar to a C−H bond *causes bond lengthening*, as discussed previously.[14a,b,18] In contrast, results from the present study suggest that 1,3-interactions between lone-pair orbitals and C−H bonds *cause bond shortening*. The above three factors, operating collectively, appear sufficient to explain qualitatively the observed behavior of C−H bond lengths in **2** as a function of ring and exocyclic C3−O3 bond conformation. Similar effects also appear to influence C−C and C−O bond lengths.

The types of structural changes observed in **2** as a function of ring and exocyclic C−O bond conformation are likely to occur in other furanose rings and thus could be important in mediating their solution behaviors and chemical/biochemical reactivities. For example, specific furanose conformations may be better "solvated" in aqueous solution not only because they assume a shape that better accommodates a solvation sphere, but because of optimization of hydrogen bond strengths (either intra- or intermolecular) *mediated by subtle adjustments of C−O bond lengths* (which affect bond polarity), the latter made possible through conformational change (Figure 6A). Likewise, the binding of a specific furanose ring conformation in an enzyme active site may result in *the proper adjustment of the electronic structure of the molecule to better accommodate the desired chemical process.* In this context, the enzyme not only supplies pertinent functional groups in proper orientation to conduct the reaction, but also in some instances adjusts the substrate structurally to take advantage of the *inherent* reactivity of the molecule. In the latter regard, protonation of the ring oxygen of a furanose ring in an enzyme-active site would restrict the conformational options of the molecule *and* induce structural changes that facilitate ring-opening *prior to* the primary chemical events. Finally, while the present discussion has been limited to the behavior of protonated furanose rings, it is possible that similar considerations may be important in enzymic reactions of other biologically-important structures.

Acknowledgment. The research reported herein was supported by the Office of Basic Energy Sciences of the United States Department of Energy, and Omicron Biochemicals, Inc. of South Bend, IN. This is Document No. NDRL-3970 from the Notre Dame Radiation Laboratory.

JA963727P

(24) Angelotti, T.; Krisko, M.; O'Connor, T.; Serianni, A. S. *J. Am. Chem. Soc.* **1987**, *109*, 4464−4472.